applied sciences

MDPI

Article

Hot Melt Extrusion as a Formulation Method of Terpolymer Rods with Aripiprazole: A Preliminary Study

Justyna Wilińska [1], Artur Turek [1,*], Jakub Rech [2], Henryk Janeczek [3], Małgorzata Pastusiak [3], Aleksandra Kordyka [3], Aleksandra Borecka [3], Magdalena Kobielarz [4] and Janusz Kasperczyk [1,3]

1 Chair and Department of Biopharmacy, Faculty of Pharmaceutical Sciences in Sosnowiec, Medical University of Silesia, Katowice, Jedności 8, 41-200 Sosnowiec, Poland; justynawilinska90@gmail.com
2 Department of Biotechnology and Genetic Engineering, Faculty of Pharmaceutical Sciences in Sosnowiec, Medical University of Silesia, Katowice, Jedności 8, 41-200 Sosnowiec, Poland; jrech@sum.edu.pl
3 Centre of Polymer and Carbon Materials, Polish Academy of Sciences, M. Curie-Skłodowskiej 34, 41-819 Zabrze, Poland; hjaneczek@cmpw-pan.edu.pl (H.J.); mpastusiak@cmpw-pan.edu.pl (M.P.); akordyka@cmpw-pan.edu.pl (A.K.); aborecka@cmpw-pan.edu.pl (A.B.); jkasperczyk@cmpw-pan.edu.pl (J.K.)
4 Department of Mechanics, Materials and Biomedical Engineering, Faculty of Mechanical Engineering, Wrocław University of Science and Technology, Wybrzeże Wyspiańskiego 27, 50-370 Wrocław, Poland; magdalena.kobielarz@pwr.edu.pl
* Correspondence: a.turek75@gmail.com or artur.turek@sum.edu.pl; Tel.: +48-32-364-12-17; Fax: +48-32-364-12-66

Abstract: Aripiprazole (ARP) is an atypical neuroleptic used in the therapy of mental diseases such as schizophrenia. The lack of optimal adherence to an oral therapy regime creates the basis for designing ARP long-acting injections. This study aimed to use 105 °C hot melt extrusion (HME) as a formulation method for rods based on poly(D,L-lactide-*co*-glycolide-*co*-trimethylene carbonate) with a molecular weight (M_n) of 21 kDa (TD,L 21), poly(L-lactide-*co*-glycolide-*co*-trimethylene carbonate) with a M_n of 59 kDa (TL 59), and with a M_n of 77 kDa (TL 77). The following methods were involved in the research: NMR, DSC, XRD, HSM, FTIR, GPC, SEM, and mechanical tests. HME at 105 °C (i) ensured flow behavior for terpolymers, (ii) did not influence the terpolymers' composition and (iii) the polymorph changes of ARP, and (iv) resulted in the changes in terpolymers' M_n. For the rods with ARP based on TD,L 21 (TD,L 21 rod-ARP) and TL 59 (TL 59 rod-ARP), plasticization was noted. No drug–terpolymer interactions were revealed. No pores were observed on the surface. Due to its high flexibility and rubber character, TD,L 21 rod-ARP may be proposed for intramuscular administration, whereas TL 59 rod-ARP, due to its higher strength and moderate stiffness, is proposed for subcutaneous administration.

Keywords: aripiprazole; drug delivery system; hot melt extrusion; implant; polymer; differential scanning calorimetry; mechanical properties; nuclear magnetic resonance; scanning electron microscopy; X-ray diffractometry

check for updates

Citation: Wilińska, J.; Turek, A.; Rech, J.; Janeczek, H.; Pastusiak, M.; Kordyka, A.; Borecka, A.; Kobielarz, M.; Kasperczyk, J. Hot Melt Extrusion as a Formulation Method of Terpolymer Rods with Aripiprazole: A Preliminary Study. *Appl. Sci.* **2023**, *13*, 9521. https://doi.org/10.3390/app13179521

Academic Editor: Roger Narayan

Received: 22 May 2023
Revised: 3 July 2023
Accepted: 4 August 2023
Published: 23 August 2023

Copyright: © 2023 by the authors. Licensee MDPI, Basel, Switzerland. This article is an open access article distributed under the terms and conditions of the Creative Commons Attribution (CC BY) license (https://creativecommons.org/licenses/by/4.0/).

1. Introduction

Aripiprazole (ARP) is among the atypical neuroleptics used to treat mental illnesses, including schizophrenia [1]. In the case of oral drug formulations, low adherence is observed, which was the reason for the development of ARP long-acting injections (ALAIs). Currently, there are only two medicinal products available that can be categorized as ALAIs, *i.e.*, Abilify Maintena® and Aristada®. However, their administration has several major disadvantages, *e.g.*, (i) the risk of pain at the injection site, (ii) no possibility of interrupting therapy, and (iii) the need to be administered on an outpatient basis [2,3]. Another problem with ALAIs is the release profile with a lag phase after administration, which requires oral supplementation [4,5].

An attempt to solve the pointed problems of the current oral therapy and ALAIs involves parenteral nano- and microformulations based on poly(lactide), poly(lactide-*co*-glycolide) (PLGA), and poly(caprolactone) [6–9]. Their formulation often requires the use of solvents, resulting in the following disadvantages: (i) a different loading efficiency for ARP depending on the composition of the polymer carrier (3.7–80.0%); (ii) different sizes of the formulation [6–9]; (iii) the risk of changes in the crystalline form of ARP [10]; (iv) the need to eliminate the residual organic solvent [11]; and (v) the decrease in the molecular weight (M_n) of the polymers [12]. Rods formulated by hot melt extrusion (HME) are an alternative solution in the processing of thermoplastic polymers. They may largely eliminate the pointed disadvantages of nano- and microformulation. HME is characterized by: (i) the high loading efficiency of the drug substance, *e.g.*, for poly(L-lactide-*co*-glycolide-*co*-trimethylene carbonate) rods with ARP it was ~94% tested previously [13]; (ii) eliminating solvents [12,14]; and (iii) the possibility of removing the formulation if side effects occur. However, HME should be also considered as the method of choice. Imparting fluidity to a thermoplastic polymer requires the use of elevated temperatures, which may cause a risk of thermal degradation of the drug substance and polymer carrier [12,14].

ARP exhibits crystalline polymorphism, including the pseudo-polymorphs and the amorphous form [10,15]. For ALAI development using the HME method, crystalline polymorphism of ARP must be taken into account to ensure the bioavailability and stability of ARP. Previously, in the study of ARP structure by proton nuclear magnetic resonance (^{1}H NMR) spectroscopy, the lack of influence of HME at 105 °C, *i.e.*, below the melting point of ARP (135.0–148.5 °C according to measurements of Braun and coworkers [16]) was determined [13].

This study aimed to use HME to formulate rods with ARP based on thermoplastic terpolymers, *i.e.*, poly(D,L-lactide-*co*-glycolide-*co*-trimethylene carbonate) with a M_n of 21 kDa (TD,L 21), poly(L-lactide-*co*-glycolide-*co*-trimethylene carbonate) with a M_n of 59 kDa (TL 59), and with a M_n of 77 kDa (TL 77). The study was carried out in several stages: (i) determination of the influence of HME conditions on the structural, thermal, and morphological properties of ARP; (ii) synthesis of TD,L 21, TL 59, and TL 77; (iii) rod formulation; and (iv) determination of the composition, thermal properties, and M_n of the terpolymers, the morphological features and mechanical properties of the rods, and (v) determination of the rate of hydrolytic degradation of rods.

2. Materials and Methods

2.1. Study of ARP

2.1.1. X-ray Diffraction Study

X-ray diffraction (XRD) patterns were obtained using a D8 Advance Diffractometer (Bruker, Karlsruhe, Germany) with a Cu-Kα cathode (λ = 1.54 Å). X-rays were generated under tube operating conditions of 40 kV and 40 mA. Measurements were carried out in the scattering range of 5–60 °C with a step size of 0.05 °C and a scan speed of 5 s/step.

Raw ARP in crystalline form III (Zhejiang Huahai Pharmaceutical Co., Ltd., Linhai China City, China) and ARP treated at 105 °C (105 °C-treated ARP) were analyzed. The 105 °C-treated ARP was prepared by heating raw ARP at 105 °C for 30 min., which reflects the conditions of HME.

The XRD patterns for raw ARP and 105 °C-treated ARP were recorded. The fitting phases were identified using the DIFFRAC.EVA program with an ICDD PDF#2 database, while lattice parameters were calculated using Rietveld refinement in the TOPAS 6 program (Bruker AXS, Karlsruhe, Germany).

2.1.2. Thermal Study

The thermal properties were analyzed by differential scanning calorimetry (DSC). The instrument (TA DSC Q2000, TA Instruments, New Castle, DE, USA) was calibrated with high-purity indium and worked under a nitrogen atmosphere (a flow rate of 50 mL/min). For raw ARP and 105 °C-treated ARP, four heating runs were performed. In the case of raw

ARP, the cooling curves were also measured. The heating and cooling runs were carried out at a rate of 20 °C/min. Analysis of the DSC curves allowed the melting temperature (T_m) and crystallization temperature (T_{cr}) to be determined.

2.1.3. Morphology Study

Hot stage microscopy (HSM) study was carried out using a polarized optical microscope (Opton Axioplan, Zeiss, Gottingen, Germany) equipped with a Nikon Coolpix 4500 camera (Nikon Corporation, Tokyo, Japan), and a hot plate (Mettler FP82, Mettler Toledo Instruments, Zurich, Switzerland) with a temperature controller (Mettler FP80, Mettler Toledo Instruments, Zurich, Switzerland). The observations of ARP were carried out in the range of 20–190 °C with images taken at 25 °C, 105 °C, 138 °C, and 140 °C (25 °C-, 105 °C-, 138 °C- and 140 °C-treated ARP, respectively).

The morphological study of ARP was performed by scanning electron microscopy (SEM) (Quanta 250 FEG/FEI, Thermo Fisher Scientific, Waltham, MA, USA) operating under low vacuum conditions (80 Pa) with an acceleration voltage of 5 kV from secondary electrons collected by a Large Field Detector. The samples prepared for SEM investigation were as follows: (i) the sample stored at 25 °C (25 °C-treated ARP); (ii) the sample heated to 105 °C (105 °C-treated ARP); and (iii) the sample heated to 140 °C (140 °C-treated ARP). Samples (ii) and (iii) were cooled by quenching.

2.2. Terpolymer Synthesis

The D,L-lactide (D,L-LA), L-lactide (L-LA), glycolide (GA), and trimethylene carbonate (TMC) were purchased from Huizhou Foryou Medical Devices Co., Ltd. (Huicheng District, Huizhou, Guangdong Province, China) and purified by recrystallization from anhydrous ethyl acetate (Sigma–Aldrich, Poznań, Poland). Zirconium (IV) acetylacetonate ($Zr(Acac)_4$) (Sigma–Aldrich, Poznań, Poland) was used as the initiator.

The TD,L 21, TL 59, and TL 77 were synthesized in bulk by the ring-opening polymerization of D,L-LA or L-LA, GA, and TMC at 120 °C for 72 h in the presence of $Zr(Acac)_4$ (initiator/monomer molar ratios of 1:600, 1:1000 and 1:1200, respectively). The synthesis of terpolymers was carried out using a pressure reactor 4848 Floor Stand Reactor (Parr Instrument Company, Moline, IL, USA) with computer control of the polymerization parameters. The obtained terpolymers were dissolved in chloroform (Avantor Performance Materials, Gliwice, Poland) and precipitated by dropwise addition into cold methanol (Avantor Performance Materials, Gliwice, Poland) with continuous stirring for purification. Finally, the terpolymers were dried under vacuum conditions at room temperature to a constant weight.

2.3. Hot Melt Extrusion

The TD,L 21, TL 59, and TL 77 terpolymers were used to formulate blank rods (TD,L 21 rod, TL 59 rod, and TL 77 rod) and rods containing 10% wt ARP (TD,L 21 rod-ARP, TL 59 rod-ARP, and TL 77 rod-ARP) using the HME process at 105 °C. Before the process, the terpolymers were dried in a vacuum at 25 °C and subjected to grinding at a temperature of −196 °C in a cryogenic mill (6870 SPEX, Thermo Fisher Scientific, Ottawa, ON, Canada). Then, the ARP was introduced into the milled terpolymers. The mixtures were vortexed for 10 min and placed in a vacuum oven (23 °C, 80 mbar) for 14 days. The terpolymers or the mixtures of terpolymer and ARP were fed into an extruder cylinder heated to 105 °C. At a value of 105 °C, the flow was obtained for terpolymers. The temperature variation was less than 1 °C during the process. This process was carried out in a co-rotating twin-screw extruder (Thermo Scientific, Haake MiniLab II, Karlsruhe, Germany) using a plasticizing screw with a constant rotational speed of 20 rpm. The molten mixture was pressed through a 0.7 mm diameter die and received on cooled rolling devices. Then, the 1 mm diameter rods were cut into 10 mm long fragments.

2.4. Study of Raw Terpolymers and Rods

2.4.1. Composition Study

The composition of raw terpolymers, blank rods, and rods with ARP was determined by ^{1}H NMR spectroscopy. Spectra were recorded using a Bruker-Avance II Ultrashield Plus spectrometer (Bruker, Karlsruhe, Germany) operating at 600 MHz using DMSO-d_6 (Sigma–Aldrich, Poznań, Poland) as a solvent with a 5.0 mm sample tube. ^{1}H NMR spectra were obtained from 32 scans, with an 11 µs pulse width and 2.65 s acquisition time. The analyses were performed at 80 °C. Parameters such as the molar percentage of lactidyl units (F_{LL}), glycolidyl units (F_{GG}), and carbonate units (F_{TMC}) were calculated according to a previously described procedure [17].

2.4.2. Thermal Study

The thermal properties of the raw terpolymers, blank rods, and rods with ARP were measured using the equipment presented in Section 2.1.2. The first heating runs (at 20 °C/min) for the initial samples and the second heating runs (at 20 °C/min) for the amorphous samples obtained by quenching from a melt in liquid nitrogen, were carried out to determine the T_m and glass transition temperature (T_g), respectively.

2.4.3. Molecular Weight Study

The M_n and molecular weight distribution (D) of the raw terpolymers, blank rods, and rods with ARP were determined by gel permeation chromatography (GPC) using a Viscotek Rimax chromatograph (Malvern Panalytical Ltd., Malvern, Worcestershire, UK) with two Viscotek 3580 columns and a Shodex SE 61 detector. The process was performed with chloroform used as a solvent (flow rate of 1 mL/min). The M_n value was calibrated with polystyrene standards.

2.4.4. Terpolymers–ARP Interaction Study

The interaction between the terpolymers and ARP was analyzed by Fourier-transform infrared spectroscopy (FTIR). The spectra were determined with a Bruker IFS 113V FTIR spectrometer (Bruker Optics Inc, Billerica, MA, USA) at an acquisition range of 4000–500 cm^{-1} (a resolution of 1 cm^{-1}). Using the solution casting method, samples were prepared from the blank rods and rods with ARP. Approximately 25 µL of 5% (w/v) terpolymer solutions in methylene chloride (Sigma–Aldrich, Poznań, Poland) were placed on a potassium bromide tablet disk. The FTIR spectra were obtained with 20 scans. Measurements were carried out at room temperature.

2.4.5. Morphology Study

The morphology observation of the blank rods and rods with ARP was performed by SEM. The study was carried out using the same methodology and SEM microscope as described in Section 2.1.3. The software ImageJ® version 1.49e (National Institutes of Health, Bethesda, MD, USA) was used for further characterization of the outer morphology. The most representative areas of the sample surface were selected for determination of heterogeneity, circularity, and solidity. The measurements were performed after calibration and conversion to binary images. The following assumptions were made: (i) a circularity value of 1.0 indicates a perfect circle; (ii) a solidity value as the area of a particle divided by its convex hull area indicates the monolithic area, where a value of 1.0 means total solidity; and (iii) heterogeneity signifies the percentage of the elevation area compared to the total area.

2.4.6. Mechanical Study

The samples for the mechanical tests were cut into 15 mm long fragments from material obtained directly after HME. Tensile tests were performed with a constant speed equal to 5 mm/min to failure using a Mecmesin MultiTest 1-i testing machine (PPT Group UK Ltd., Slinfold, West Sussex, UK). Engineering stress and strain were calculated, and the

stress–strain characteristics, $\sigma = f(\varepsilon)$, were determined. According to the standard PN-EN ISO 527-1:2020-01, the following mechanical parameters were calculated: Young's modulus (E); yield stress and strain (σ_y, ε_y); breaking stress and strain (σ_b, ε_b); and maximum stress and strain (σ_m, ε_m).

2.4.7. Rod Hydrolytic Degradation Study

The TD,L 21 rod, TL 59 rod, and TL 77 rod were placed in a solution of phosphate-buffered saline (pH 7.4) (Sigma–Aldrich, Poznań, Poland) and incubated under constant conditions (37 °C; 240 rpm). Changes in the water uptake (*WU*) and weight loss (*WL*) of the rods were determined using Equations (1) and (2), respectively:

$$WU\ (\%) = (\text{wet mass} - \text{dry mass})/(\text{dry mass}) \times 100 \quad (1)$$

$$WL\ (\%) = (\text{initial mass} - \text{dry mass})/(\text{dry mass}) \times 100 \quad (2)$$

3. Results and Discussion

3.1. Structural Characterization of ARP

ARP belongs to the substances which represent conformational polymorphism [10,16]. In this study, form III of ARP, which is determined as metastable in the entire temperature range and is marketed in medicinal products the most often, was used in the formulation process. Braun and coworkers revealed the conversions between crystalline forms of ARP using solutions of form III in water and mixtures of water with acetonitrile, ethanol, methanol, or tetrahydrofuran [10,16].

HME utilizing the thermoplastic properties of polymers and eliminating the solvent was applied. Braun and coworkers also pointed out that heating form III above the T_m and keeping it at about 145 °C can favor conversion to form I [16]. Therefore, carrying out the formulation process below the T_m of ARP should guarantee the maintenance of form III, and thus the bioavailability and stability of the drug substance. In this study, the structural and thermal characterizations were made for raw ARP and 105 °C-treated ARP to determine the HME conditions (Figures 1–4, Tables 1 and 2).

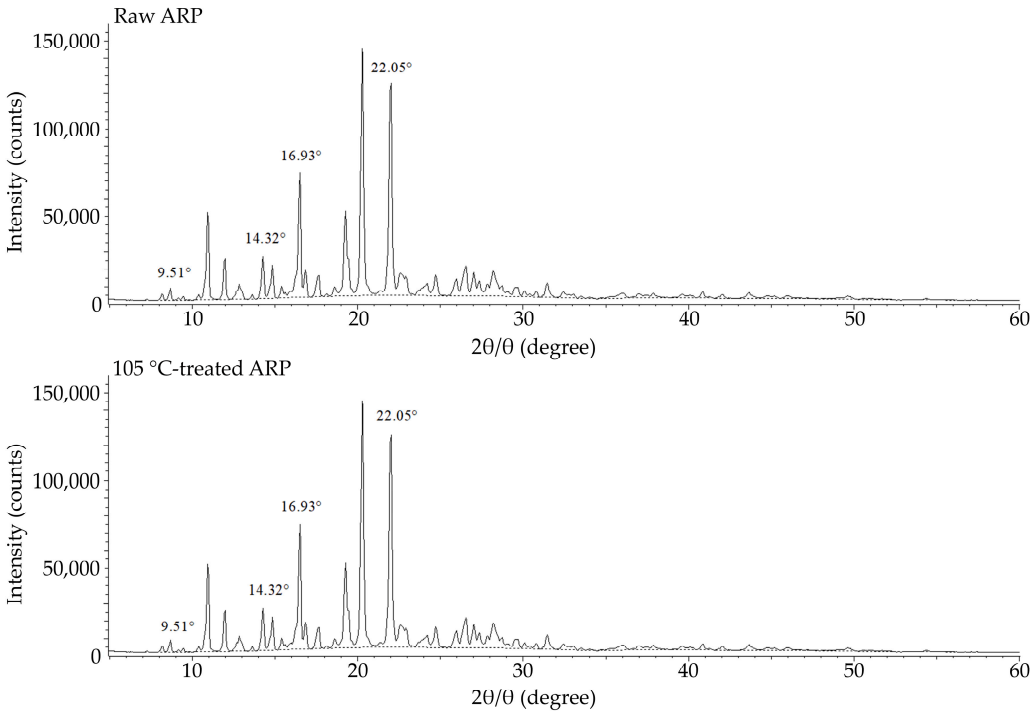


Figure 1. Diffraction pattern of raw ARP and 105 °C-treated ARP.

Table 1. Calculated lattice parameters of raw ARP and 105 °C-treated ARP.

Sample	Lattice Parameters [Å]						Cell Volume (Å 3)	Crystal System
	a (Å)	b (Å)	c (Å)	A (°)	β (°)	γ (°)		
Raw ARP	10.161	12.143	18.714	82.197	82.570	82.863	2,255.213	Triclinic
105 °C-treated ARP	10.163	12.142	18.714	82.189	82.570	81.863	2,255.219	Triclinic

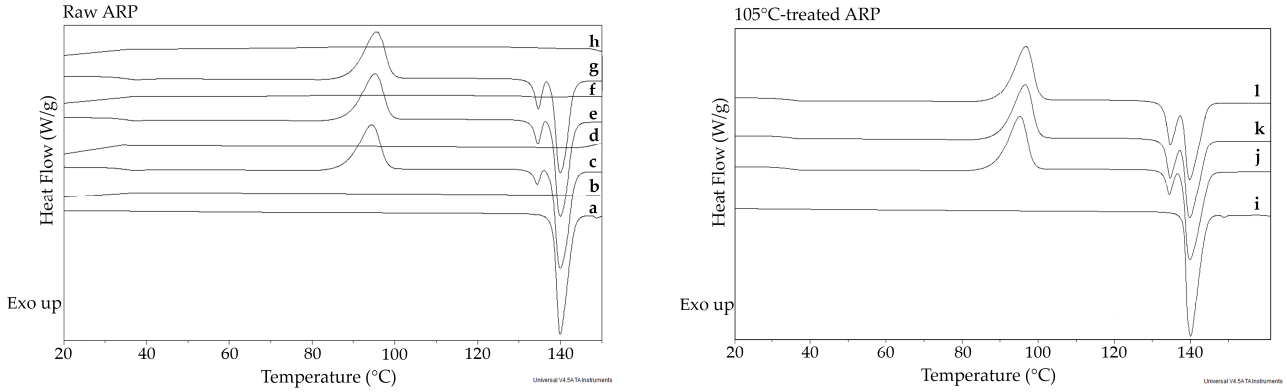


Figure 2. The DSC heating curves for raw ARP for the first (**a**), second (**c**), third (**e**), and fourth (**g**) heating runs. The DSC cooling curves after the first (**b**), second (**d**), third (**f**), and fourth heating runs (**h**). The DSC heating curves for 105 °C-treated ARP for the first (**i**), second (**j**), third (**k**), and fourth heating runs (**l**).

Table 2. The thermal parameters characterizing raw ARP and 105 °C-treated ARP during the four heating runs.

	Heating Run	T_{m1} (°C)	ΔH_1 (J/g)	T_{m2} (°C)	ΔH_2 (J/g)	T_{cr} (°C)	ΔH_{cr} (J/g)
Raw ARP	First	*ND*	*ND*	140.0	95.7	*ND*	*ND*
	Second	134.4	7.2	140.0	90.1	94.4	91.8
	Third	134.7	7.6	139.9	90.5	95.6	90.2
	Fourth	134.8	7.5	139.9	90.7	96.6	90.2
105 °C-treated ARP	First	*ND*	*ND*	140.1	95.7	*ND*	*ND*
	Second	134.6	7.6	139.9	91.8	95.2	91.8
	Third	139.6	5.4	139.6	91.1	95.6	90.9
	Fourth	134.7	6.5	139.9	90.5	96.6	90.2

T_{m1} and T_{m2}—melting temperatures, ΔH_1 and ΔH_2—enthalpies of melting, T_{cr}—crystallization temperature, ΔH_{cr}—enthalpy of crystallization, *ND*—non-detected.

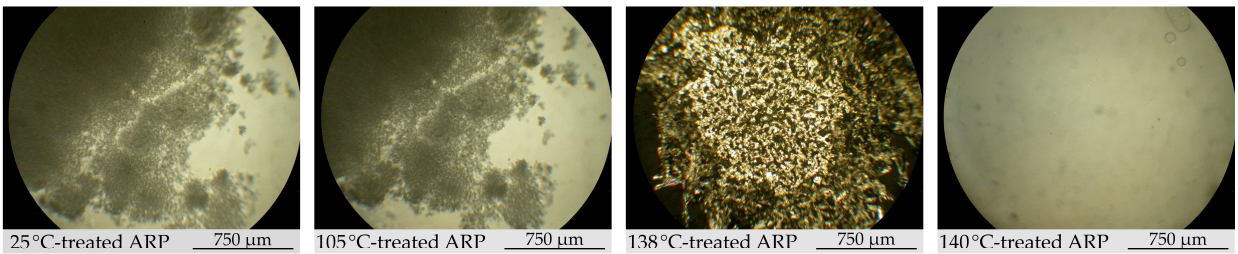


Figure 3. HSM images of 25 °C-treated ARP, 105 °C-treated ARP, 138 °C-treated ARP, and 140 °C-treated ARP.

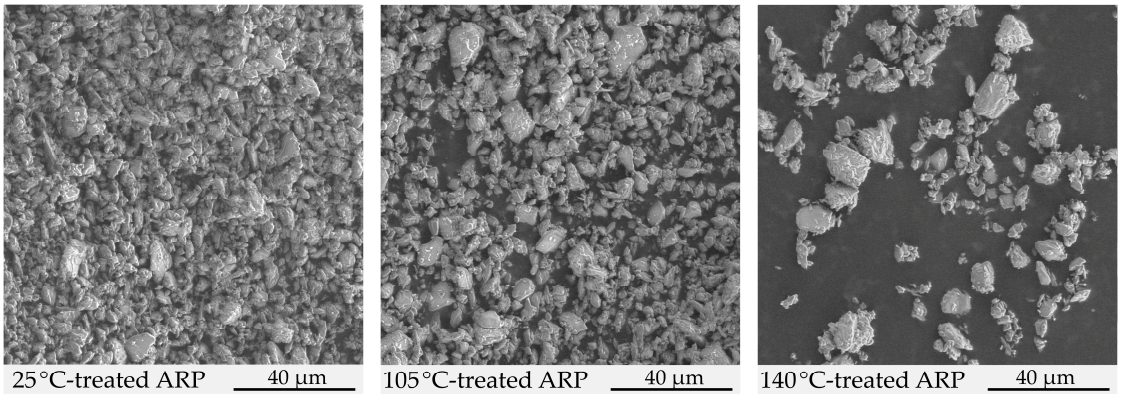


Figure 4. SEM images of 25 °C-treated ARP, 105 °C-treated ARP, and 140 °C-treated ARP.

In the XRD study, form III of ARP was confirmed according to the manufacturer's declaration (Zhejiang Huahai Pharmaceutical Co., Ltd., Linhai China City, China). The characteristic peaks for form III, including 9.51°, 14.32°, 16.93°, and 22.05°, were revealed for both raw ARP and 105 °C-treated ARP. Moreover, the spectrum for the 105 °C-treated ARP sample did not reveal changes, which may confirm the lack of a phase transition (Figure 1 and Table 1).

A DSC study was performed to potentially provide further information about possible changes during the formulation process (Figure 2 and Table 2). Four heating runs of raw ARP and 105 °C-treated ARP samples were carried out. Additionally, raw ARP cooling curves were also monitored. Two DSC heating runs for raw ARP showed typical effects for crystalline substances. Analysis of the first and second heating runs revealed the melting point at 140.0 °C (95.7 J/g) and the crystallization effect at 94.4 °C (91.8 J/g), respectively (Figure 2 and Table 2). The value of the T_m from the first heating run reflected the T_m obtained by Braun and coworkers for form III [16]. Next, double-melting endotherms at 134.4 °C (7.2 J/g) and 140.0 °C (90.1 J/g) (Figure 2 and Table 2) may suggest transformation to forms IV and III after crystallization, respectively [16]. However, the transformation of form III to a mixture of forms III and IV by heating and cooling was not confirmed by other methods. This is also not described in the literature and it is also beyond the aim of this study. The third and fourth heating runs revealed the same thermal events. Analysis of the cooling of raw ARP at 20 °C/min after all the heating runs also did not reveal significant thermal events (Figure 2 and Table 2), which may indicate slow kinetics of crystallization. The data obtained suggest that HME at 105 °C allowed the crystalline form III of ARP to remain. The study of the 105 °C-treated ARP did not show significant differences compared to the raw ARP. The DSC analysis of raw ARP and 105 °C-treated ARP revealed the same crystalline character for the drug substance (Figure 2 and Table 2), which confirms the thermal stability during HME.

The DSC measurement of ARP reflects the morphological observations performed by HSM and SEM. In the HSM study, the raw ARP sample was heated from 20 °C to 190 °C. The images were recorded at 25 °C, 105 °C, 138 °C, and 140 °C (Figure 3). The 25 °C-treated ARP showed the crystalline character of raw ARP. The 105 °C-treated ARP revealed maintenance of the crystalline structure and no polymorph conversion. In turn, for the 138 °C-treated ARP, the birefringence of ARP crystals was observed, while the 140 °C-treated ARP showed an amorphous and homogenous state of ARP without phase separation (Figure 3).

In the SEM study, analogous observations were revealed. The samples were prepared differently than for HSM due to the specifics of the SEM imaging. The 105 °C-treated ARP and 140 °C-treated ARP samples were heated and rapidly cooled. The 25 °C-treated ARP and 105 °C-treated ARP revealed their crystalline character. A lack of significant morphological changes for the 105 °C-treated ARP confirmed the stability of ARP at 105 °C.

The treatment of ARP samples at 140 °C and rapid cooling resulted in the crystallization of ARP into larger crystalline forms (Figure 4).

All measurements pointed to the fact that APR may safely be thermally processed below its T_m. Therefore, the selection of polymer carriers should take this into account in the case of formulation by HME.

3.2. Characterization of Raw Terpolymers

In the case of PLGA copolymers, features such as the composition considering lactide stereoisomeric forms and the value of M_n are indicated as some of the most important in the design of a drug formulation [18]. In this study, three terpolymers based on D,L-LA or L-LA, GA, and TMC with F_{LL} in the range of 57.1–65.4 mol%, F_{GG} in the range of 14.7–18.3 mol%, and F_{TMC} in the range of 18.9–24.6 mol% with M_n of 21.4, 59.4, and 76.8 kDa were synthesized (Figure 5 and Table 3). The application of terpolymers containing TMC as drug carriers may significantly change the features of drug carriers in the areas of matrix degradation, release, and the bioavailability of drug substances in comparison to PLGA copolymers [18–24].

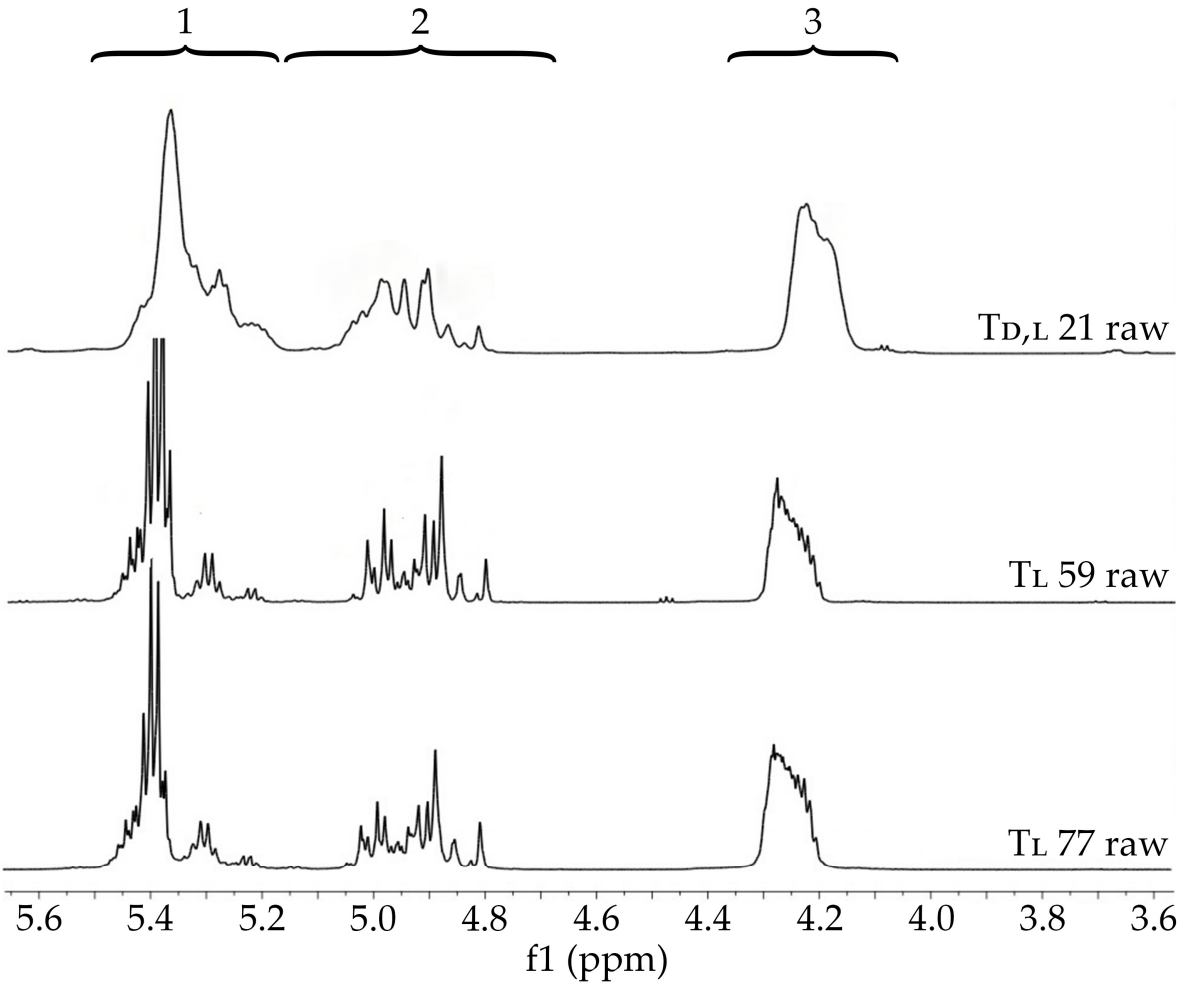


Figure 5. ^{1}H NMR spectra of raw terpolymers (TD,L 21 raw, TL 59 raw, and TL 77 raw) (600 MHz, DMSO-d_6, 80 °C). ^{1}H NMR spectra: the proton region of the lactidyl units (1), the methylene proton region of the glycolidyl (2), and carbonate units (3).

Table 3. The parameters characterizing raw terpolymers (TD,L 21 raw, TL 59 raw, and TL 77 raw), blank rods (TD,L 21 rod, TL 59 rod, and TL 77 rod) and rods with ARP (TD,L 21 rod-ARP; TL 59 rod-ARP; and TL 77 rod-ARP).

Sample		F_{LL} (mol%)	F_{GG} (mol%)	F_{TMC} (mol%)	T_m (°C)	ΔH (J/g)	T_g (°C)	M_n (kDa)	D
TD,L 21	Raw	65.4	14.7	19.9	*ND*	*ND*	36.3	21.4	1.970
	Rod	63.9	15.7	20.4	*ND*	*ND*	35.1	20.4	2.030
	rod-ARP	63.5	15.9	20.6	128.7	8.4	33.7	18.7	1.998
TL 59	Raw	64.9	16.2	18.9	*ND*	*ND*	46.7	59.4	1.950
	Rod	64.9	16.2	18.9	*ND*	*ND*	44.1	57.7	1.604
	rod-ARP	65.4	16.3	18.3	133.4	5.2	41.8	55.2	2.012
TL 77	Raw	57.1	18.3	24.6	*ND*	*ND*	39.9	76.8	2.001
	Rod	56.2	18.3	25.5	*ND*	*ND*	37.3	46.8	2.301
	rod-ARP	56.2	18.3	25.5	133.6	3.4	37.4	43.9	1.928

F_{LL}—molar percentage of lactidyl units in the terpolymer, F_{GG}—molar percentage of glycolidyl units in the terpolymer, F_{TMC}—molar percentage of carbonate units in the terpolymer, T_m—melting temperature, ΔH—value of enthalpy, T_g—glass transition temperature, M_n—molecular weight, D—molecular weight distribution, *ND*—non-detected.

Generally, PLGA copolymers with L-LA are semi-crystalline with a clear endothermal event on the DSC curve indicating the phenomenon of melting [21]. In this study, the DSC curves did not reveal melting endotherms for all terpolymers (Figure 6 and Table 3), which may suggest an amorphous character of all the obtained terpolymers. This feature may ensure higher bioavailability compared to semi-crystalline material. This attribute was suggested in the previous study of P(LA:GA:TMC) terpolymers releasing 17-β-estradiol and aripiprazole [13,22].

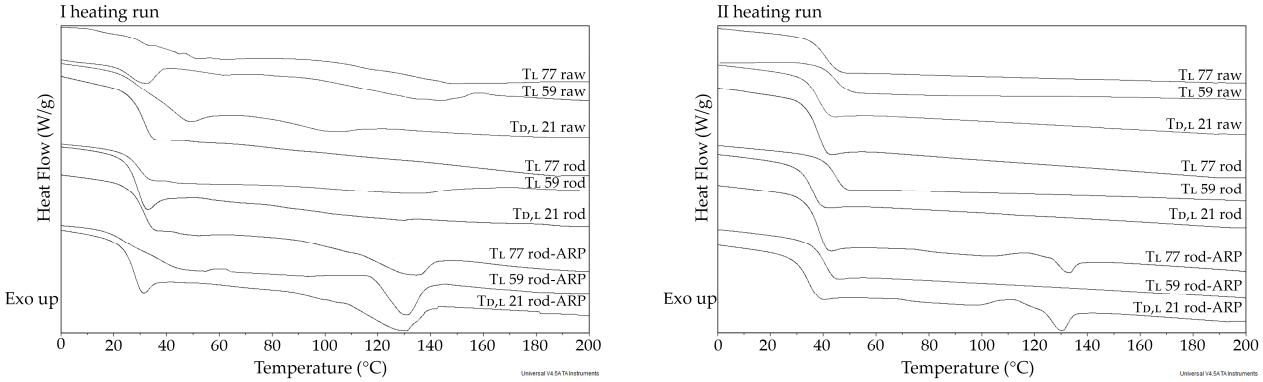


Figure 6. The DSC curves of the first and second heating runs for raw terpolymers (TD,L 21 raw, TL 59 raw, and TL 77 raw), blank rods (TD,L 21 rod, TL 59 rod, and TL 77 rod), and rods with ARP (TD,L 21 rod-ARP, TL 59 rod-ARP, and TL 77 rod-ARP).

In the case of PLGA copolymers, the value of the M_n is an important parameter to tailor the release profile of drug substances [18]. Generally, a lower M_n increases hydrophilicity, faster *WU* and degradation. Therefore, this study aimed to design rods with ARP based on terpolymers with various M_n values, *i.e.*, 21 kDa, 59 kDa, and 77 kDa. It should be pointed out that an appropriately higher M_n value of terpolymers based on D,L-LA, L-LA, GA, and TMC is difficult to obtain. Therefore, in this study, $Zr(Acac)_4$ was proposed as a polymerization initiator providing the possibility of synthesizing polymers with a higher M_n than can be obtained with the commonly used tin(II) 2-ethylhexanoate ($Sn(Oct)_2$). Generally, increasing the amount of monomers relative to the amount of initiator results in an increase in the M_n [25].

In this study, terpolymers with a M_n of 21 kDa, 59 kDa, and 77 kDa were synthesized with initiator/monomer ratios of 1:600, 1:1000, and 1:1200, respectively (Table 3). Moreover, $Zr(Acac)_4$ is less toxic than $Sn(Oct)_2$, which was shown previously [25].

The accepted view is that the T_g value should be above the physiological temperature of the human body. Then, it is assumed that the formulation remains as a solid because of the glassy state. However, this may inhibit the release of drug substances [26]. In this study, the T_g for the synthesized terpolymers was in the range of 36.3–46.7 °C. The lowest value of the T_g was determined for the terpolymer with D,L-LA, *i.e.*, 36.3 °C (Figure 6 and Table 3). A T_g close to human body temperature may result in a shorter lag phase.

3.3. Characterization of the Rods and Rod with ARP

3.3.1. Terpolymer Composition

The HME and the introduction of ARP did not influence the terpolymer composition (Figure 7 and Table 3), which reflects previous studies [12,13,22,27].

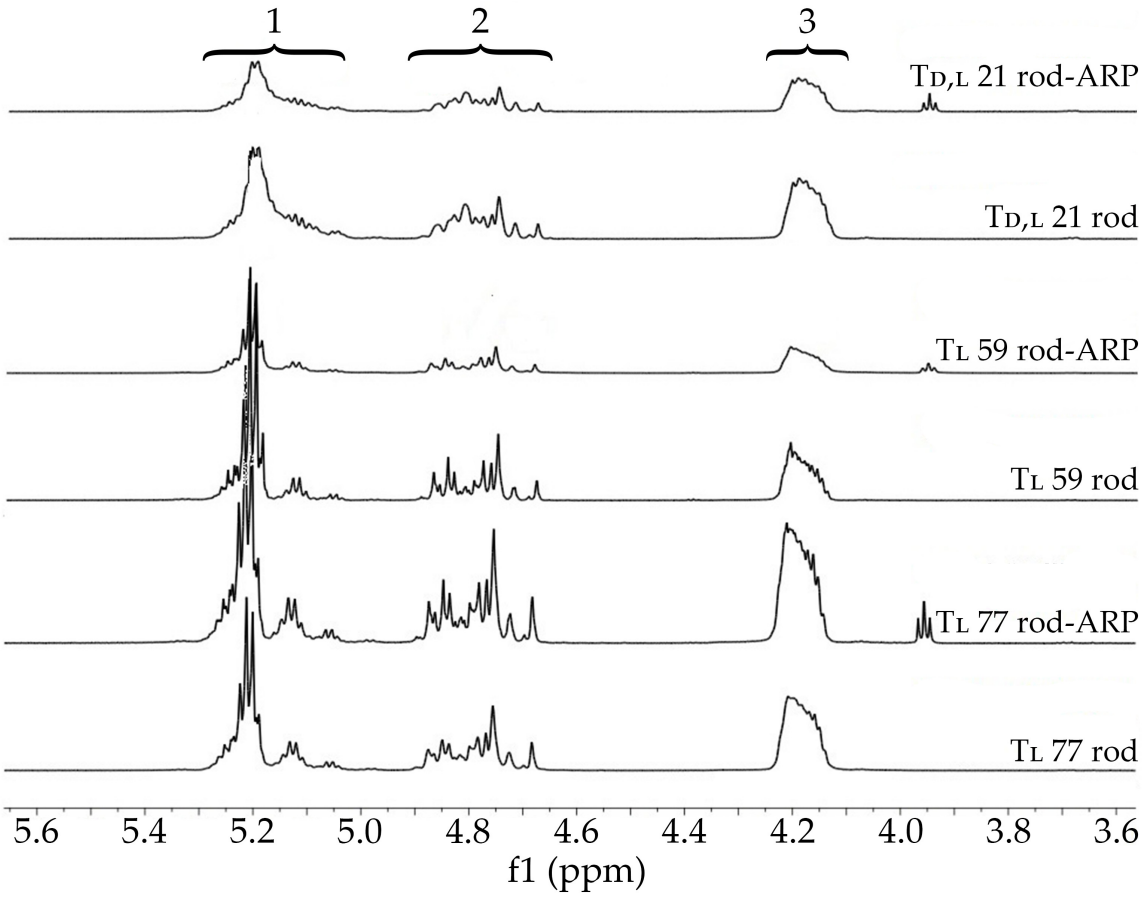


Figure 7. The ^{1}H NMR spectra of blank rods (TD,L 21 rod, TL 59 rod, and TL 77 rod) and rods with ARP (TD,L 21 rod-ARP, TL 59 rod-ARP, and TL 77 rod-ARP) (600 MHz, DMSO-d6, 80 °C). ^{1}H NMR spectra: the proton region of the lactidyl units (1), the methylene proton region of the glycolidyl (2), and carbonate units (3).

3.3.2. Thermal Study

Analysis of the DSC curves representing the first heating runs for the TD,L 21 rod, TL 59 rod, and TL 77 rod also did not reveal clear endotherms (Figure 6 and Table 3), which indicated the unchanged crystallographic state of the terpolymers in the blank rods after HME. However, for the TD,L 21 rod-ARP, TL 59 rod-ARP, and TL 77 rod-ARP, clear endotherms in the first heating run at 128.7 °C, 133.4 °C, and 133.6 °C (respectively) were revealed, which shows the presence of ARP. The peaks observed for the rods with ARP possessed lower values compared to raw ARP (140 °C) (Figure 2 and Table 2). Moreover, these were less intense and less sharp (Figure 6). Considering the data obtained from the XRD (Figure 1 and Table 1), DSC (Figure 2 and Table 2), HSM (Figure 3), and SEM

(Figure 4) studies on the structural characterization of ARP after HME, the difference between the T_m value of the identified form III of ARP (Figure 2 and Table 2) and the T_m of the rod-ARP (Figure 6 and Table 3) results from a relatively small amount of drug substance in the polymer carrier. It is an orderly and stable arrangement of two phases, *i.e.*, crystalline APR suspended in the amorphous terpolymer. It should be pointed out that in the second heating run for the TD,L 21 rod-ARP and TL 77 rod-ARP, endotherms at 130.3 °C (1.728 J/g) and 132.4 °C (0.705 J/g), respectively, were also observed (Figure 6). This may evidence the restoration of the orderly arrangement after amorphization of the samples during quenching. However, for the TL 59 rod-ARP, the endothermic peak was absent, which may suggest the ARP was in an amorphous state or in a disordered crystalline phase of molecular dispersion in the polymer matrix. A similar conclusion was indicated by Mainardes and coworkers for praziquantel-loaded poly(D,L-lactide-*co*-glycolide) (D,L-PLGA) nanoparticles in which one interpretation of the lack of an endotherm in the first heating run was that the drug was in an amorphous state or in a disordered crystalline phase of molecular dispersion in the PLGA polymeric matrix [28].

Analysis of the second heating runs revealed that the T_g of terpolymers is below the T_m of ARP. In addition, the terpolymers also have a flow temperature below the T_m of ARP. This makes it possible to formulate rods based on the synthesized thermoplastic terpolymers by HME at 105 °C without changing the crystallographic properties of form III of ARP. Moreover, analysis of the second heating runs revealed the well-known thermal phenomena for formulated rods showing that the formulation of blank rods did not reveal important changes for the stability of the formulation. The decrease in the T_g was revealed in the range of 1.2–2.6 °C comparing raw terpolymers and blank rods (Figure 6 and Table 3). The literature data point to the fact that the T_g decrease as a result of HME at a temperature above 100 °C is related to short-term hydrolytic degradation caused by the presence of moisture [29]. However, it should be noted that during the first heating run in this study, water evaporation as a flat endotherm was not revealed (Figure 6). The presence of oxygen in thermal degradation during HME is also not insignificant. It should be pointed out that the total elimination of moisture and oxygen is practically impossible [12,29]. Furthermore, the plasticization effect for the TD,L 21 rod-ARP and TL 59 rod-ARP was noted because of the decrease in the T_g (1.4 °C and 2.3 °C, respectively) (Figure 6 and Table 3). Generally, plasticizers are a separate group of compounds [30], but the drug substances themselves may also have a plasticizing effect, *e.g.*, indomethacin and PLGA [31]. It should be noted that plastification caused by ARP during HME may also facilitate the formulation process of poly(L-lactide-*co*-glycolide-*co*-trimethylene carbonate) terpolymers. Moreover, ARP as a plasticizer may be used with high T_g polymers to facilitate the release of drug substances, which may accelerate the release process.

3.3.3. M_n Study

This study revealed the influence of the HME process on the decrease in the M_n value of terpolymers based on D,L-LA or L-LA, GA, and TMC. This issue has already been extensively discussed in previous studies. The decrease in the M_n of poly(D,L-lactide-*co*-glycolide-*co*-trimethylene carbonate) and poly(L-lactide-*co*-glycolide-*co*-trimethylene carbonate) was 41.68% and 24.15%, respectively [12]. For comparison, other authors revealed a M_n decrease in the range of 27–69% during melt processing for poly(D,L-lactide), poly(L-lactide), D,L-PLGA, and poly(L-lactide-*co*-glycolide) (L-PLGA) [32–40]. The literature also points out the shearing forces caused by the rotating screw during HME as a reason for the M_n decrease in aliphatic polyesters [33–35,37,38,40].

In this study, the noted changes reflect the pertinent literature data. A decrease in M_n in the range of 2.9–39.1% for blank rods was noted. Less susceptible to a M_n decrease were blank rods based on terpolymers with a lower initial value, *i.e.*, the TD,L 21 rod and TL 59 rod. The highest loss of M_n was observed for the TL 77 rod (39.1%, *i.e.*, 30 kDa). The introduction of ARP resulted in a decrease in M_n, which was insignificant from the point of view of formulation stability (Table 3).

3.3.4. Terpolymer-ARP Interaction Study

The analysis of the FTIR spectra of all the blank rods revealed the following signals: (i) at 3015 cm^{-1} (stretching of CH), (ii) at 1757 cm^{-1} (stretching of C=O), (iii) in the range of 1500–1350 cm^{-1} (deformations of CH_3), (iv) in the range of 1300–1000 cm^{-1} (stretching of C–O), (v) at 933 cm^{-1} (deformations of CH), and (vi) at 878 cm^{-1} (deformations of CH). The spectra for the rods with ARP (TD,L 21 rod-ARP, TL 59 rod-ARP, and TL 77 rod-ARP) did not show significant differences in the signals revealed (Figure 8), which suggests the lack of interactions between the terpolymers and ARP.

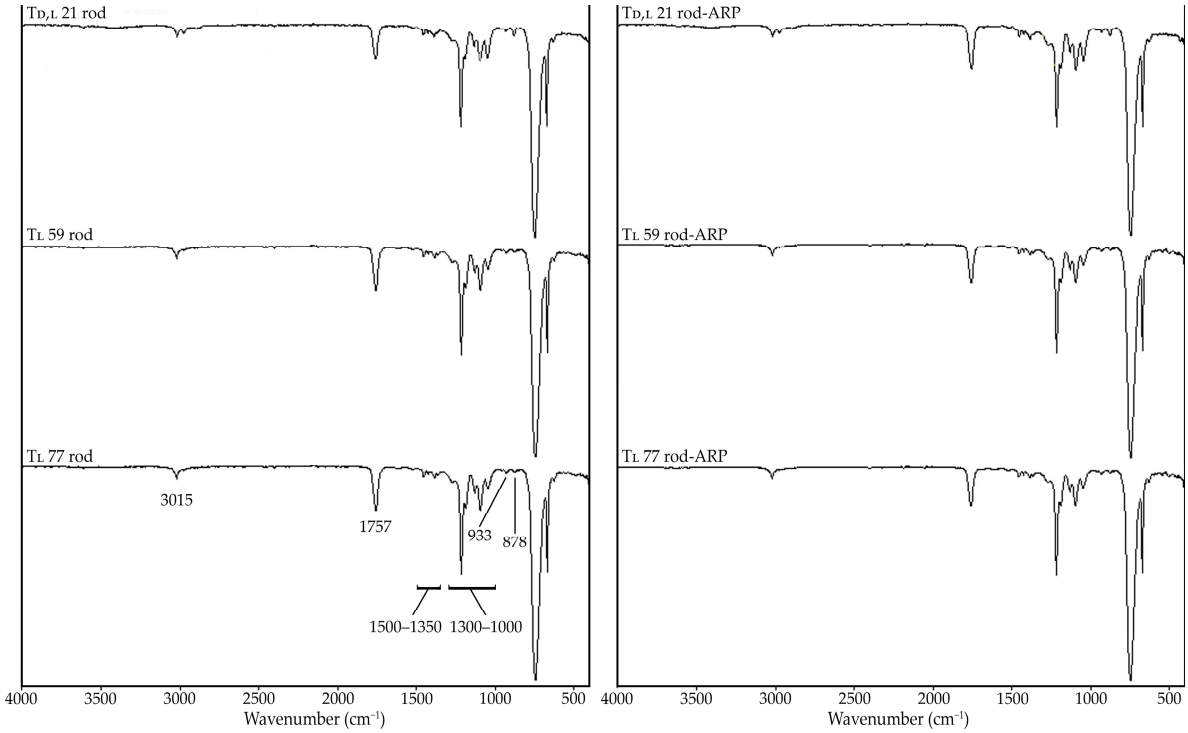


Figure 8. The FTIR spectra of blank rods (TD,L 21 rod, TL 59 rod, and TL 77 rod) and rods with ARP (TD,L 21 rod-ARP, TL 59 rod-ARP, and TL 77 rod-ARP) in the range of 4000–500 cm^{-1}.

These findings reflect the DSC study. The first and second heating runs of the blank rods and the rods with ARP (Figure 6 and Table 3) did not reveal additional endotherms and exotherms except those identified as crystalline ARP (Figure 2), which also indicates the lack of interaction between ARP and the terpolymers. In another study of the physical mixture of ARP and D,L-PLGA, the DSC curves also did not reveal additional thermal events [41]. According to the literature, the absence of additional endothermic or exothermic peaks is interpreted as indicating a lack of drug–polymer interactions [42,43].

3.3.5. Morphology Study

The characterization of rod morphology based on SEM images (Figure 9) analyzed by ImageJ® software revealed the differences in the heterogeneity between blank rods and rods with ARP, whereas, for the circularity and solidity, the presence of a drug substance did not play an important role (Table 4).

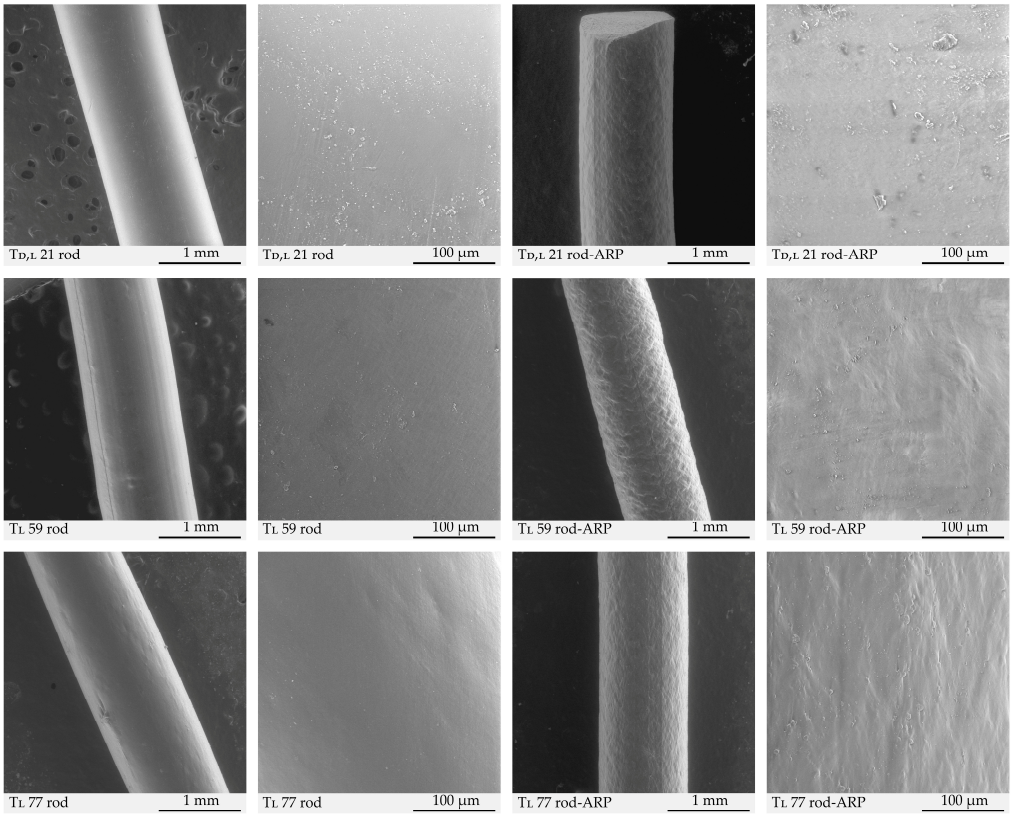


Figure 9. SEM images of blank rods (TD,L 21 rod, TL 59 rod, and TL 77 rod) and rods with ARP (TD,L 21 rod-ARP, TL 59 rod-ARP, and TL 77 rod-ARP).

Table 4. Heterogeneity, circularity, and solidity for the images with the scale bar equal to 100 µm of blank rods (TD,L 21 rod, TL 59 rod, and TL 77 rod) and rods with ARP (TD,L 21 rod-ARP, TL 59 rod-ARP, and TL 77 rod-ARP) calculated by ImageJ®.

Sample		Area (µm^2)	Heterogeneity (%)	Circularity	Solidity
TD,L 21	rod	35,394.7	12.9	0.043	0.83
	rod-ARP	35,492.7	19.9	0.042	0.85
TL 59	rod	35,871.9	16.5	0.039	0.81
	rod-ARP	35,179.7	36.5	0.039	0.83
TL 77	rod	35,611.1	15.5	0.039	0.85
	rod-ARP	35,719.9	23.6	0.029	0.87

Previously, it was revealed that the presence of risperidone or ARP influenced the increase in morphological diversity of implantable rods based on poly(lactide-*co*-glycolide-*co*-trimethylene carbonate) terpolymers [12,13]. In this study, the thesis presented in the literature was developed by calculations using ImageJ® software. The introduction of ARP into the terpolymer matrix increased the rod heterogeneity from a range of 12.9–16.5% to a range of 19.9–36.5% (Table 4).

A lack of pores was observed for blank rods and rods with ARP (Figure 9) and confirmed by a low rate of circularity (0.029–0.043) (Table 4). It should be added that the value of 1.0 for the circularity means perfect circles, which would indicate the presence of pores. These observations may result from both the formulation method and polymer properties. It should be pointed out that because of the melting of the polymer material, HME does not cause the formation of pores [12,13,22,27]. In the case of injectable extruded D,L-PLGA rods with N-acetylcysteine, no porosity was observed either [44]. The outer morphology of the extruded formulation reflects more the topography of the inner surface of the die in the extruder than the properties of the polymer. Moreover, the features of

the P(LA:GA:TMC) terpolymers used point to a more amorphous character, which may also be the cause of the lack of pores. In contrast, for the matrices based on L-PLGA with risperidone formulated by the solution-casting method, pores were observed. Pore formation was observed for semi-crystalline polymers processed by low-temperature methods [21]. A lack of pores in the native rods seems to be an advantageous feature from the administration point of view because pores may significantly weaken the rod structure during implantation with a pre-filled syringe. Huang and coworkers have shown that the increase in porosity of the D,L-PLGA films incorporated with poly(ethylene glycol) could have contributed to the decrease in tensile strength [45].

In this study, the HME process did not result in unfavorable changes in the formulation's morphology. Disintegration, cracks, microcavities, and slits were not observed (Figure 9), which was reflected by the high values of solidity (Table 4), *i.e.*, 0.81–0.87, where the value of 1 means the monolithic area.

3.3.6. Mechanical Study

In this study, the influence of the terpolymer composition, M_n, and the presence of ARP in the rods on the mechanical properties was determined under tensile loadings (Figure 10 and Table 5).

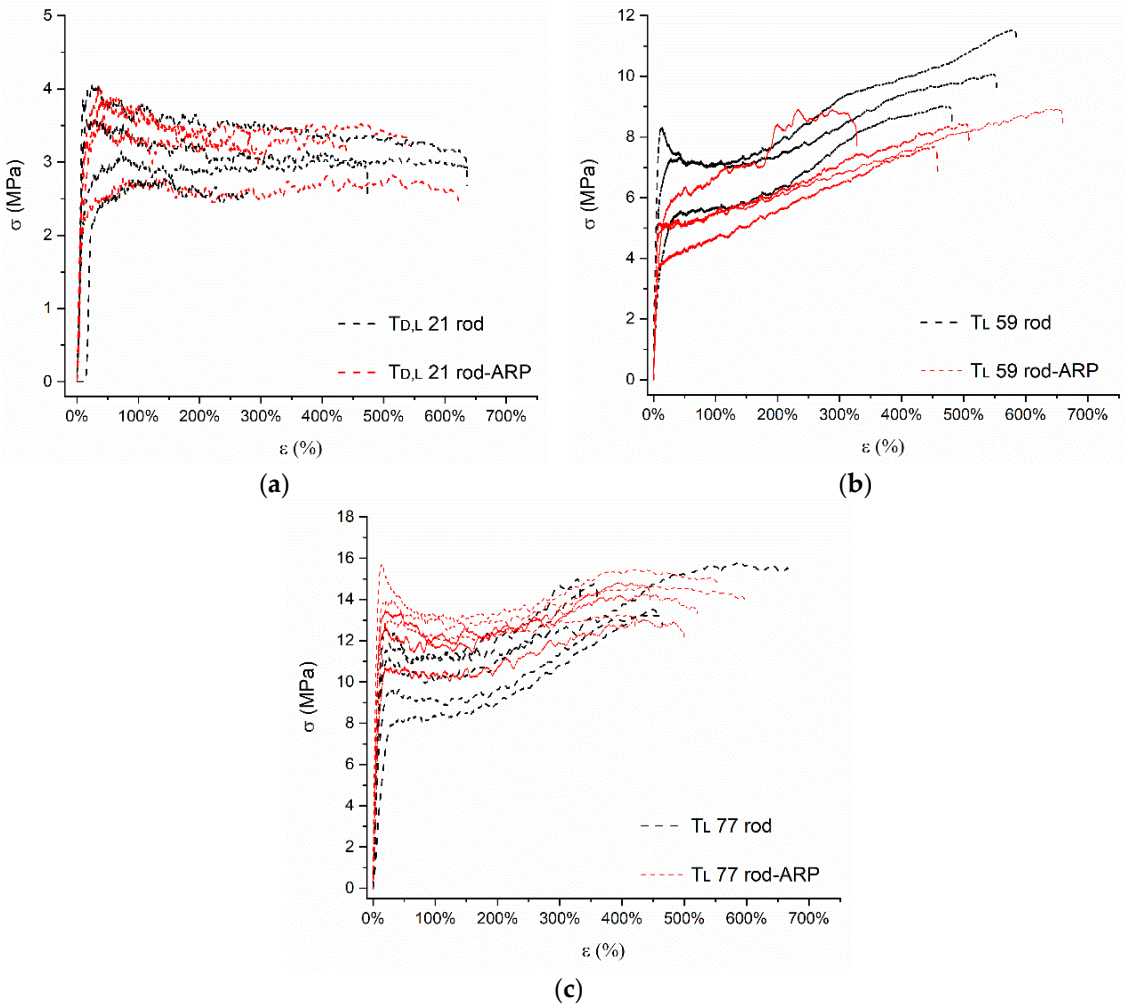


Figure 10. Exemplary stress–strain ($\sigma = f(\varepsilon)$) curves determined for blank rods and rods with ARP: (**a**) TD,L 21 rod and TD,L 21 rod-ARP, (**b**) TL 59 rod and TL 59 rod-ARP; and (**c**) TL 77 rod and TL 77 rod-ARP.

Table 5. Mechanical parameters of blank rods and rods with ARP (±SD).

Sample		σ_y (MPa)	ε_y (%)	σ_m (MPa)	ε_m (%)	σ_b (MPa)	ε_b (%)	E (MPa)
TD,L 21	rod	4.21 ± 1.14	20.3 ± 10.9	4.32 ± 1.10	108.0 ± 138.5	3.20 ± 0.78	488.8 ± 118.5	62.03 ± 28.33
	rod-ARP	3.62 ± 0.58	28.0 ± 9.8	3.77 ± 0.50	101.0 ± 152.0	2.62 ± 0.29	402.0 ± 157.7	18.90 ± 7.96
TL 59	rod	7.04 ± 1.39	28.3 ± 16.0	10.20 ± 1.26	533.2 ± 57.1	9.64 ± 1.36	539.7 ± 53.3	194.92 ± 100.21
	rod-ARP	5.15 ± 1.01	23.0 ± 19.1	8.48 ± 0.58	460.3 ± 173.7	7.58 ± 0.74	488.5 ± 137.2	128.67 ± 33.52
TL 77	rod	10.67 ± 1.71	28.4 ± 7.6	14.44 ± 1.07	436.4 ± 100.2	13.28 ± 1.36	456.4 ± 131.3	85.01 ± 22.09
	rod-ARP	13.24 ± 1.61	18.7 ± 4.1	14.30 ± 0.97	350.3 ± 167.1	13.12 ± 1.02	507.0 ± 67.1	221.94 ± 88.04

σ_y—yield stress, ε_y—yield strain, σ_m—maximum stress, ε_m—strain stress, σ_b—breaking stress, ε_b—breaking strain, E—Young's modulus.

The stress–strain curves ($\sigma = f(\epsilon)$) for the analyzed formulations showed the ductile modes of deformation, classified according to the PN-EN ISO 527-1:2020-01 standard, as types B and C. Type B was distinctive for the curves of the TL 59 rod and TL 59 rod-ARP, and the TL 77 rod and TL 77 rod-ARP. Strain hardening after crossing the yield point was noted for all type B curves. After crossing the yield point, stresses initially decreased and subsequently increased to failure at the highest stress values. Type C was noted for curves of the TD,L 21 rod and TD,L 21 rod-ARP when the values of yield (σ_y) and maximum stresses (σ_m) were comparable. For type C curves, stresses slightly decreased and remained relatively constant until failure of the material (Figure 10).

The analysis of mechanical parameters, such as σ_y, ε_y, σ_m, ε_m, σ_b, and E, showed these to be lower for rods based on TD,L 21 compared to rods based on TL 59 and TL 77 (Table 5). These results indicate a significant relationship of the mechanical properties with LA stereochemistry and the value of the M_n. The density of the TD,L 21 chain packing was lower than for TL 59 and TL 77. Amorphous regions of TD,L 21 weakened the mechanical properties, whereas for TL 59 and TL 77, the interactions between L-LA chains enhanced the mechanical stability of the formulations. Moreover, shorter chains of TD,L 21 may have been the deciding factor in weakening mechanical properties.

The presence of ARP in terpolymers resulted in weakening the mechanical properties of the formulations. For the TD,L 21 rod-ARP, the value of E was significantly lower compared to the TD,L 21 rod, which indicates the lower stiffness of the TD,L 21 rod-ARP, whereas the presence of the drug substance in the TL 59 rod-ARP caused a decrease in all the analyzed mechanical parameters. The TL 59 rod-ARP had less strength and was less stiff and deformable at all stages of stretching than the TL 59 rod. It should be pointed out that the DSC study revealed that the plasticization effect (Figure 6 and Table 3) resulting from the presence of ARP in the TD,L 21 rod-ARP and TL 59 rod-ARP may be connected with the reduction in mechanical properties. The plasticization of D,L-PLGA caused by wetting the D,L-PLGA scaffolds with water or ethanol resulted in the same effect [46]. The comparison of the TL 77 rod-ARP and TL 77 rod revealed that the presence of the drug substance caused the most significant differences in mechanical behavior; the formulation became significantly stiffer (E = 221.94 ± 88.04 MPa and 85.01 ± 22.09 MPa, respectively) and less extensible (ε_y = 18.7 ± 4.1% vs. 28.4 ± 7.6% and ε_m = 350.3 ± 167.1% vs. 436.4 ± 100.2%, respectively). It could be pointed out that the presence of ARP blurred the rubbery and flexible behavior of TMC, despite the highest content of this component (~25%) (Table 3). However, it should be added that the ARP did not act as a plasticizer in the case of the TL 77 rod-ARP (Figure 6 and Table 3). Other failure parameters are comparable for TL 77 rod and TL 77 rod-ARP (Table 5).

From the mechanical point of view, the most promising formulation for subcutaneous administration is the TL 59 rod-ARP due to its higher strength and moderate stiffness, whereas, for intramuscular administration, the TD,L 21 rod-ARP seems to be the most appropriate because of its high flexibility and rubbery character. In terms of mechanical properties, the TL 77 rod-ARP is the least promising. However, it should be pointed out that the study of rods with 17-β-estradiol based on poly(L-lactide-*co*-glycolide-*co*-trimethylene carbonate) with a similar composition (57.9:17.6:24.5) and M_n (45.8 kDa) performed on adult

female Wistar rats did not reveal inflammation, necrosis, or exudate after subcutaneous implantation in the back of the neck [22].

3.3.7. Rod Hydrolytic Degradation Study

The hydrolytic degradation of aliphatic polyesters and polycarbonates is a result of the hydrolysis of ester bonds. A favorable phenomenon of this process is the *WU*. It should also be underlined that direct proof for hydrolytic degradation is the *WL*. The changes in the polymer content, T_g, and M_n provide only data about the structural changes of degradable aliphatic polyesters and polycarbonates [13,18–22,47].

In this study of significant relationships of *WU* and *WL* with LA stereochemistry, the value of the T_g and M_n were also shown. In the case of rods based on TD,L 21, the most dynamic changes in *WU* and *WL* (Figure 11) were facilitated by the amorphous regions of LA, the lowest values T_g ensuring the highest chain mobility, and the lowest M_n responsible for the shortest polymer chains. The longest degradation period was noted for the TL 59 rod, in which *WU* and *WL* were the slowest resulting from the highest T_g and M_n (Table 3).

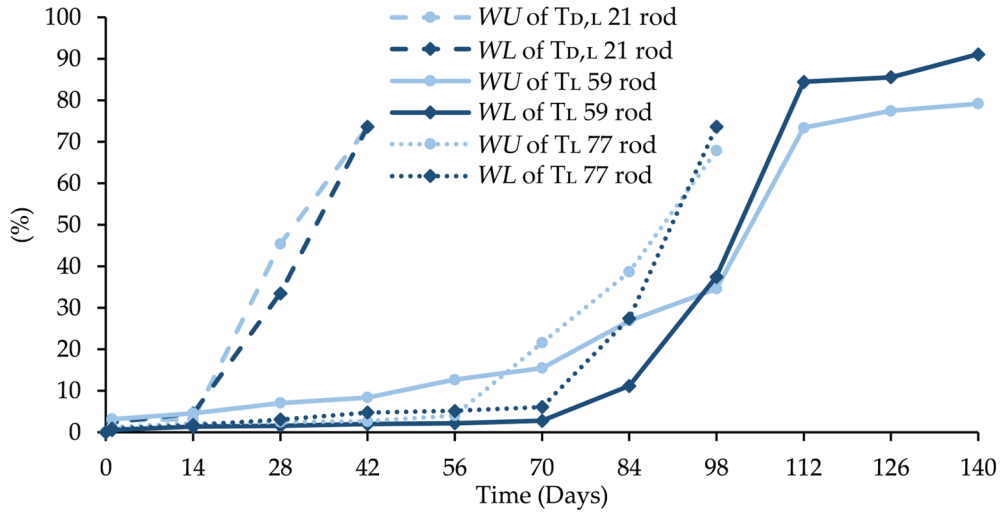


Figure 11. Changes (%) in water uptake (*WU*), and weight loss (*WL*) during the degradation of TD,L 21 rod, TL 59 rod, and TL 77 rod.

4. Conclusions

Rods with ARP based on D,L-LA or L-LA, GA, and TMC terpolymers with a M_n of 21 kDa, 59 kDa, and 77 kDa were formulated. The determining factor for the terpolymer's M_n, synthesized in bulk by the ring opening polymerization, was the ratio of the monomer to the polymerization initiator.

The temperature of 105 °C during HME ensured flow behavior for the applied terpolymers. Simultaneously, nothing of concern was observed in the properties of the ARP and terpolymers. The structural, thermal, and morphological properties of form III of ARP used were maintained, and the conversion into other crystalline forms did not take place. HME did not influence the composition of the terpolymers. However, it resulted in changes in the M_n without destabilizing the formulations. Furthermore, the observed plasticization effect for the TD,L 21 rod-ARP rod and TL 59 rod-ARP may have facilitated the formulation process. The DSC and FTIR studies did not show drug–terpolymer interactions. From the mechanical point of view, the most promising formulation for intramuscular administration, the TD,L 21 rod-ARP, seems to be the most appropriate because of its high flexibility and rubbery character, whereas for subcutaneous administration a better option is the TL 59 rod-ARP due to its higher strength and moderate stiffness.

HME is the appropriate method for the formulation of ALAIs based on D,L-LA or L-LA, GA, and TMC terpolymers with a M_n of 21 kDa, 59 kDa, and 77 kDa.

Author Contributions: Conceptualization, A.T.; methodology, A.T., J.W., A.B., M.K., H.J., M.P., A.K. and J.K.; validation, A.T., A.B., M.K., H.J., M.P. and A.K.; formal analysis, A.T., J.W., H.J., M.K. and A.B.; investigation, A.T., J.W., J.R., A.B., H.J., M.K., M.P. and A.K.; resources, A.T. and J.W.; data curation, A.T., J.W., J.R., A.B., M.K. and H.J.; writing—original draft preparation, A.T., J.W. and M.K.; writing—review and editing, A.T. and J.R.; visualization, A.T., J.W. and J.R.; supervision, A.T.; project administration, A.T.; funding acquisition, A.T. All authors have read and agreed to the published version of the manuscript.

Funding: This work was supported by the Medical University of Silesia in Katowice (grant numbers PCN-1-066/N/1/F and PCN-1-010/K/2/F).

Institutional Review Board Statement: Not applicable.

Informed Consent Statement: Not applicable.

Data Availability Statement: The data presented in this study are available on request from the corresponding author.

Acknowledgments: Aripiprazole was kindly donated by Przedsiębiorstwo Farmaceutyczne LEKAM Sp. z o.o., Poland. The graphical abstract was partly generated using Servier Medical Art (https://smart.servier.com, accessed on 28 June 2023), provided by Servier, licensed under a Creative Commons Attribution 3.0 unported license.

Conflicts of Interest: The authors declare no conflict of interest.

References

1. Casey, A.B.; Canal, C.E. Classics in chemical neuroscience: Aripiprazole. *ACS Chem. Neurosci.* **2017**, *8*, 1135–1146. [CrossRef]
2. Biagi, E.; Capuzzi, E.; Colmegna, F.; Mascarini, A.; Brambilla, G.; Ornaghi, A.; Santambrogio, J.; Clerici, M. Long-acting injectable antipsychotics in schizophrenia: Literature review and practical perspective, with a focus on aripiprazole once-monthly. *Adv. Ther.* **2017**, *34*, 1036–1048.
3. Frampton, J.E. Aripiprazole lauroxil: A review in schizophrenia. *Drugs* **2017**, *77*, 2049–2056. [CrossRef] [PubMed]
4. Shirley, M.; Perry, C.M. Aripiprazole (ABILIFY MAINTENA®): A review of its use as maintenance treatment for adult patients with schizophrenia. *Drugs* **2014**, *74*, 1097–1110. [CrossRef] [PubMed]
5. Hard, M.L.; Mills, R.J.; Sadler, B.M.; Turncliff, R.Z.; Citrome, L. Aripiprazole lauroxil: Pharmacokinetic profile of this long-acting injectable antipsychotic in persons with schizophrenia. *J. Clin. Psychopharmacol.* **2017**, *37*, 289–295. [CrossRef] [PubMed]
6. Talegaonkar, S.; Mittal, A.; Parmar, S.; Aqil, M. Aripiprazole loaded polymeric biodegradable microspheres: Formulation and in vitro characterization. *J. Dispers. Sci. Technol.* **2009**, *30*, 1198–1202. [CrossRef]
7. Babu, A.C.; Babu, P.K.; Sudhakar, K.; Subha, M.C.; Rao, K.C. Aripiprazole loaded PLGA nanoparticles for controlled release studies: Effect of co-polymer ratio. *Int. J. Drug Deliv.* **2014**, *6*, 151–155.
8. Hiraoka, S.; Uchida, S.; Namiki, N. Preparation and characterization of high-content aripiprazole-loaded core-shell structure microsphere for long-release injectable formulation. *Chem. Pharm. Bull.* **2014**, *62*, 654–660. [CrossRef]
9. Sawant, K.; Pandey, A.; Patel, S. Aripiprazole loaded poly(caprolactone) nanoparticles: Optimization and in vivo pharmacokinetics. *Mater. Sci. Eng. C Mater. Biol. Appl.* **2016**, *66*, 230–243. [CrossRef]
10. Braun, D.E.; Gelbrich, T.; Kahlenberg, V.; Tessadri, R.; Wieser, J.; Griesser, U.J. Stability of solvates and packing systematics of nine crystal forms of the antipsychotic drug aripiprazole. *Cryst. Growth Des.* **2009**, *9*, 1054–1065. [CrossRef]
11. Kamali, H.; Atamanesh, M.; Kaffash, E.; Mohammadpour, F.; Khodaverdi, E.; Hadizadeh, F. Elimination of residual solvent from PLGA microspheres containing risperidone using supercritical carbon dioxide. *J. Drug Deliv. Sci. Technol.* **2020**, *57*, 101702. [CrossRef]
12. Turek, A.; Borecka, A.; Janeczek, H.; Sobota, M.; Kasperczyk, J. Formulation of delivery systems with risperidone based on biodegradable terpolymers. *Int. J. Pharm.* **2018**, *548*, 159–172. [CrossRef] [PubMed]
13. Turek, A.; Rech, J.; Borecka, A.; Wilińska, J.; Kobielarz, M.; Janeczek, H.; Kasperczyk, J. The role of the mechanical, structural, and thermal properties of poly(L-lactide-co-glycolide-co-trimethylene carbonate) in the development of rods with aripiprazole. *Polymers* **2021**, *13*, 3556. [CrossRef] [PubMed]
14. Stanković, M.; Frijlink, H.W.; Hinrichs, W.L. Polymeric formulations for drug release prepared by hot melt extrusion: Application and characterization. *Drug. Discov. Today* **2015**, *20*, 812–823.
15. Łaszcz, M.; Witkowska, A. Studies of phase transitions in the aripiprazole solid dosage form. *J. Pharm. Biomed. Anal.* **2016**, *117*, 298–303. [CrossRef]
16. Braun, D.E.; Gelbrich, T.; Kahlenberg, V.; Tessadri, R.; Wieser, J.; Griesser, U.J. Conformational polymorphism in aripiprazole: Preparation, stability and structure of five modifications. *J. Pharm. Sci.* **2009**, *98*, 2010–2026. [CrossRef]
17. Gębarowska, K.; Kasperczyk, J.; Dobrzyński, P.; Scandola, M.; Zini, E.; Li, S. NMR analysis of the chain microstructure of biodegradable terpolymers with shape memory properties. *Eur. Polym. J.* **2011**, *47*, 1315–1327. [CrossRef]

18. Fredenberg, S.; Wahlgren, M.; Reslow, M.; Axelsson, A. The mechanisms of drug release in poly(lactic-co-glycolic acid)-based drug delivery systems—A review. *Int. J. Pharm.* **2011**, *415*, 34–52. [CrossRef]
19. Albertsson, A.C.; Eklund, M. Influence of molecular structure on the degradation mechanism of degradable polymers: In vitro degradation of poly(trimethylene carbonate), poly(trimethylene carbonate-co-caprolactone), and poly(adipic anhydride). *J. Appl. Polym. Sci.* **1995**, *57*, 87–103. [CrossRef]
20. Pêgo, A.P.; Poot, A.A.; Grijpma, D.W.; Feijen, J. In vitro degradation of trimethylene carbonate based (co)polymers. *Macromol. Biosci.* **2002**, *2*, 411–419. [CrossRef]
21. Turek, A.; Kasperczyk, J.; Jelonek, K.; Borecka, A.; Janeczek, H.; Libera, M.; Gruchlik, A.; Dobrzyński, P. Thermal properties and morphology changes in degradation process of poly(L-lactide-co-glycolide) matrices with risperidone. *Acta Bioeng. Biomech.* **2015**, *17*, 11–20.
22. Turek, A.; Olakowska, E.; Borecka, A.; Janeczek, H.; Sobota, M.; Jaworska, J.; Kaczmarczyk, B.; Jarząbek, B.; Gruchlik, A.; Libera, M.; et al. Shape-memory terpolymer rods with 17-β-estradiol for the treatment of neurodegenerative diseases: An in vitro and in vivo study. *Pharm. Res.* **2016**, *33*, 2967–2978.
23. Zhang, Y.; Liang, R.; Xu, J.; Shen, L.; Gao, J.; Wang, X.; Wang, N.; Shou, D.; Hu, Y. Efficient induction of antimicrobial activity with vancomycin nanoparticle-loaded poly(trimethylene carbonate) localized drug delivery system. *Int. J. Nanomed.* **2017**, *12*, 1201–1214. [CrossRef] [PubMed]
24. Turek, A.; Stoklosa, K.; Borecka, A.; Paul-Samojedny, M.; Kaczmarczyk, B.; Marcinkowski, A.; Kasperczyk, J. Designing biodegradable wafers based on poly(L-lactide-co-glycolide) and poly(glycolide-co-ε-caprolactone) for the prolonged and local release of idarubicin for the therapy of glioblastoma multiforme. *Pharm. Res.* **2020**, *37*, 90. [CrossRef] [PubMed]
25. Czajkowska, B.; Dobrzynski, P.; Bero, M. Interaction of cells with L-lactide/glycolide copolymers synthesized with the use of tin or zirconium compounds. *J. Biomed. Mater. Res. A* **2005**, *74*, 591–597. [CrossRef]
26. Liu, G.; McEnnis, K. Glass transition temperature of PLGA particles and the influence on drug delivery applications. *Polymers* **2022**, *14*, 993. [CrossRef]
27. Olakowska, E.; Właszczuk, A.; Turek, A.; Borecka, A.; Liśkiewicz, A.; Wawro, D.; Kasperczyk, J.; Jędrzejowska-Szypułka, H.J. Effects of 17-β-estradiol released from shape-memory terpolymer rods on sciatic nerve regeneration after injury and repair with chitosan nerve conduit in female rats. *Appl. Biomed.* **2022**, *20*, 87–97.
28. Mainardes, R.M.; Gremião, M.P.; Evangelista, R.C. Thermoanalytical study of praziquantel-loaded PLGA nanoparticles. *Rev. Bras. Cienc. Farm.* **2006**, *42*, 523–530. [CrossRef]
29. Ellä, V.; Nikkola, L.; Kellomäki, M. Process-induced monomer on a medical-grade polymer and its effect on short-term hydrolytic degradation. *J. Appl. Polym. Sci.* **2011**, *119*, 2996–3003. [CrossRef]
30. Snejdrova, E.; Drastik, M.; Dittrich, M.; Kastner, P.; Nguyenova, J. Mucoadhesive plasticized system of branched poly(lactic-co-glycolic acid) with aciclovir. *Drug. Dev. Ind. Pharm.* **2016**, *42*, 1653–1659. [CrossRef]
31. Prudic, A.; Lesniak, A.K.; Ji, Y.; Sadowski, G. Thermodynamic phase behaviour of indomethacin/PLGA formulations. *Eur. J. Pharm. Biopharm.* **2015**, *93*, 88–94. [CrossRef] [PubMed]
32. Cicero, J.A.; Dorgan, J.R. Physical properties and fiber morphology of poly(lactic acid) obtained from continuous two-step melt spinning. *J. Polym. Environ.* **2001**, *9*, 1–10. [CrossRef]
33. Gogolewski, S.; Jovanovic, M.; Perren, S.M.; Dillon, J.G.; Hughes, M.K. The effect of melt-processing on the degradation of selected polyhydroxyacids: Polylactides, polyhydroxybutyrate, and polyhydroxybutyrate-co-valerates. *Polym. Degrad. Stab.* **1993**, *40*, 313–322. [CrossRef]
34. Carrasco, F.; Pagès, P.; Gámez-Pérez, J.; Santana, O.O.; Maspoch, M.L. Processing of poly(lactic acid): Characterization of chemical structure, thermal stability and mechanical properties. *Polym. Degrad. Stab.* **2010**, *95*, 116–125.
35. Nuutinen, J.P.; Clerc, C.; Virta, T.; Törmälä, P. Effect of gamma, ethylene oxide, electron beam, and plasma sterilization on the behaviour of SR-PLLA fibres in vitro. *J. Biomater. Sci. Polym. Ed.* **2002**, *13*, 1325–1336. [CrossRef]
36. Rothen-Weinhold, A.; Besseghir, K.; Gurny, R. Analysis of the influence of polymer characteristics and core loading on the in vivo release of a somatostatin analogue. *Eur. J. Pharm. Biopharm.* **1997**, *5*, 303–313.
37. Rothen-Weinhold, A.; Besseghir, K.; Vuaridel, E.; Sublet, E.; Oudry, N.; Kubel, F.; Gurny, R. Injection-molding versus extrusion as manufacturing technique for the preparation of biodegradable implants. *Eur. J. Pharm. Biopharm.* **1999**, *48*, 113–121.
38. Simpson, R.L.; Nazhat, S.N.; Blaker, J.J.; Bismarck, A.; Hill, R.; Boccaccini, A.R.; Hansen, U.N.; Amis, A.A. A comparative study of the effects of different bioactive fillers in PLGA matrix composites and their suitability as bone substitute materials: A thermo-mechanical and in vitro investigation. *J. Mech. Behav. Biomed. Mater.* **2015**, *50*, 277–289.
39. Yen, H.J.; Tseng, C.S.; Hsu, S.H.; Tsai, C.L. Evaluation of chondrocyte growth in the highly porous scaffolds made by fused deposition manufacturing (FDM) filled with type II collagen. *Biomed. Microdevices* **2009**, *11*, 615–624.
40. Yuan, X.; Mak, A.F.; Kwok, K.W.; Yung, B.K.; Yao, K. Characterization of poly(L-lactic acid) fibers produced by melt spinning. *J. Appl. Polym. Sci.* **2001**, *81*, 251–260. [CrossRef]
41. Nakashima, A.; Izumi, T.; Ohya, K.; Kondo, K.; Niwa, T. Design of highly dispersible PLGA microparticles in aqueous fluid for the development of long-acting release injectables. *Chem. Pharm. Bull.* **2017**, *65*, 157–165. [CrossRef]
42. Gao, L.; Li, Q.; Zhang, J.; Huang, Y.; Deng, L.; Li, C.; Tai, G.; Ruan, B. Local penetration of doxorubicin via intrahepatic implantation of PLGA based doxorubicin-loaded implants. *Drug Deliv.* **2019**, *26*, 1049–1057. [CrossRef]

43. He, P.; Xu, S.; Guo, Z.; Yuan, P.; Liu, Y.; Chen, Y.; Zhang, T.; Que, Y.; Hu, Y. Pharmacodynamics and pharmacokinetics of PLGA-based doxorubicin-loaded implants for tumor therapy. *Drug Deliv.* **2022**, *29*, 478–488. [CrossRef] [PubMed]
44. Desai, K.G.; Mallery, S.R.; Schwendeman, S.P. Formulation and characterization of injectable poly(DL-lactide-co-glycolide) implants loaded with N-acetylcysteine, a MMP inhibitor. *Pharm. Res.* **2008**, *25*, 586–597. [CrossRef] [PubMed]
45. Huang, C.L.; Steele, T.W.; Widjaja, E.; Boey, F.Y.; Venkatraman, S.S.; Loo, J.S. The influence of additives in modulating drug delivery and degradation of PLGA thin films. *NPG Asia Mater.* **2013**, *5*, e54. [CrossRef]
46. Wu, L.; Zhang, J.; Jing, D.; Ding, J. "Wet-state" mechanical properties of three-dimensional polyester porous scaffolds. *J. Biomed. Mater. Res. A* **2006**, *76*, 264–271. [CrossRef] [PubMed]
47. Borecka, A.; Rech, J.; Janeczek, H.; Wilińska, J.; Kasperczyk, J.; Kobielarz, M.; Grieb, P.; Turek, A. Development of the latanoprost solid delivery system based on poly(l-lactide-co-glycolide-co-trimethylene carbonate) with shape memory for glaucoma treatment. *Appl. Sci.* **2023**, *13*, 7562. [CrossRef]

Disclaimer/Publisher's Note: The statements, opinions and data contained in all publications are solely those of the individual author(s) and contributor(s) and not of MDPI and/or the editor(s). MDPI and/or the editor(s) disclaim responsibility for any injury to people or property resulting from any ideas, methods, instructions or products referred to in the content.